Case 18416

Eurorad

Myriad findings of multisystem-radiological-manifestations in a case of Erdheim–Chester disease

Published on 04.01.2024

DOI: 10.35100/eurorad/case.18416
ISSN: 1563-4086
Section: Neuroradiology
Area of Interest: Cardiovascular system CNS Musculoskeletal system
Procedure: Biopsy
Procedure: Chemotherapy
Imaging Technique: CT
Imaging Technique: MR
Imaging Technique: PET-CT
Special Focus: Haematologic diseases Neoplasia Pathology Case Type: Clinical Case
Authors: Shilna Thuppilikattu 1, Varun Narayan 1, Sreeraj V. 2, Geetha C.G. 3
Patient: 44 years, male

Clinical History:

A 44-year-old man with no known comorbidities presented with bilateral lower limb oedema and right-sided proptosis associated with decreased vision for the last year. Loss of appetite and weight loss were present for three months. On examination, he had ascites. Laboratory tests showed no remarkable findings

Imaging Findings:

Xanthelasma of right eyelid noted (Figure 1). Orbit-MRI revealed heterogeneously enhancing T2WI-hypointense soft-tissue thickening involving bilateral extraocular muscles, intraconal spaces with right-sided proptosis and compression of bilateral optic nerves (Figures 2a, 2b). Axial post-contrast T1WI image showed an enhancing focus in left peridentate nucleus region (Figure 2b) and enhancing thickening involving bilateral tentorium cerebelli (Figure 2c). Optic disc drusens were noted in both eyes (Figures 3a, 3b). Axial-CT demonstrated sclerotic bone thickening of bilateral ethmoidal and sphenoidal sinuses (Figure 3a). T2WI-hypointense soft-tissue and wall thickening of paranasal sinuses (Figures 4a, 4c) showed heterogeneous post-contrast enhancement (Figures 4b, 4d). T2WI-hypointense lobulated lesion (Figure 5a) with increased FDG-uptake (Figure 5b) involving choroid plexus in right occipital horn showing homogenous post-contrast enhancement (Figure 5c) was noted. Sagittal non-contrast T1WI image demonstrated absence of posterior pituitary bright spot (Figure 6). USG-neck showed perivascular thickening in right carotid bulb (Figure 7). Cardiac-MRI showed soft-tissue thickening involving walls of both atria, atrioventricular groove, right coronary artery and left circumflex artery (Figure 8a), showing late gadolinium enhancement (Figure 8b). FDG-avid diffuse retroperitoneal soft-tissue thickening encasing kidneys and bilateral moderate hydroureteronephrosis (Figures 9a, 9b) was noted. Intense FDG-uptake was observed in bilateral testis (Figure 10). Radiographs of bilateral knee joints demonstrated FDG-avid symmetrical metadiaphyseal osteosclerosis (Figures 11a, 11b).

Discussion:

Erdheim-Chester Disease (ECD) is a multisystemic non-Langerhans cell histiocytic disorder seen in adults between 40 and 70 years [1], which manifests with diverse clinical symptoms like bone pain (most common) [2], exophthalmos, xanthomas, cerebellar signs, dyspnoea, diabetes insipidus and constitutional symptoms [3] posing a diagnostic dilemma for clinicians. Our case illustrates various imaging manifestations in all organ systems. Pathognomic features of skeletal involvement include bilateral symmetric-metadiaphyseal osteosclerosis, cortical thickening, and increased FDG-uptake in long bones, predominantly lower limbs, sparing epiphysis and axial skeleton [4,5]. Patients with neurologic involvement carry a poor prognosis and are an independent predictor of death [3,6]. The absence of high signal intensity of posterior pituitary on non-contrast sagittal T1W-image [7] was observed in our case. Meningeal lesions [8], bilateral symmetric T2-hyperintense lesions in the dentate and cerebellar hemisphere with no post-contrast enhancement [8,9] and involvement of choroid plexus of lateral ventricles [10] have been described in ECD. Increased meningeal enhancement and thickening in bilateral tentorium cerebelli, basitemporal region, along cavernous sinus and an asymmetric enhancing focus in the left peridentate nucleus along with T2WI hypointense lobulated lesion with increased FDG-uptake showing homogenous post-contrast enhancement involving choroid plexus of right occipital horn were noted in our case. Orbital involvement occurs in the form of bilateral enhancing intraconal/extraconal masses with/without optic nerve compression [11]. Paranasal sinus involvement occurs in the form of sinus wall osteosclerosis [8] and FDG-avid heterogeneously enhancing soft-tissue thickening [5]. Bilateral optic-drusens, as noted in our case, have been reported very rarely [3]. Cardiovascular involvement carries a poor prognosis, and it can manifest as pericardial infiltration, myocardial infiltration of the atrioventricular wall, atrial (predominantly right), interatrial septum with late gadolinium enhancement [12] and increased FDG-uptake. This was demonstrated in our case using cardiac-MRI. Vascular involvement, described in previous studies as form of periadventitial soft-tissue infiltration of the aorta, predominantly infra-renal abdominal aorta, bilateral common carotid arteries, subclavian arteries, pulmonary trunk and visceral arteries, predominantly renal artery [13], was also noted in our case. Pulmonary manifestations like nodules and interlobular septal thickening [14], as described in previous cases, were not seen in our case. Our study revealed only subsegmental atelectatic bands and pleural effusion as pleuropulmonary manifestations. Retroperitoneal involvement occurs in the form of bilateral symmetric perirenal and pararenal infiltration, resulting in the 'hairy kidney sign' and involvement of the proximal ureter [12]. Increased FDG-uptake noted in bilateral testis is very rare in ECD [15]. The final diagnosis of ECD was made based on a biopsy from upper tibial lesion with immunohistochemistry (CD68-positive and CD1a-negative) and a positive $BRAF^{V600E}$ mutation [1]. The patient was treated with steroids and vinblastine, but unfortunately, the patient succumbed to sepsis after starting treatment.

All patient data have been completely anonymised throughout the entire manuscript and related files.

Differential Diagnosis List: Erdheim-Chester disease with multisystem involvement, Langerhans cell histiocytosis, Lymphoma, IgG4-related disease, Sarcoidosis, Retroperitoneal fibrosis

Final Diagnosis: Erdheim-Chester disease with multisystem involvement

References:

Diamond EL, Dagna L, Hyman DM, Cavalli G, Janku F, Estrada-Veras J, Ferrarini M, Abdel-Wahab O, Heaney ML, Scheel PJ, Feeley NK, Ferrero E, McClain KL, Vaglio A, Colby T, Arnaud L, Haroche J (2014) Consensus guidelines for the diagnosis and clinical management of Erdheim-Chester disease. Blood 124(4):483-92. doi: 10.1182/blood-2014-03-561381. (PMID: 24850756)

Breuil V, Brocq O, Pellegrino C, Grimaud A, Euller-Ziegler L (2002) Erdheim-Chester disease: typical radiological bone features for a rare xanthogranulomatosis. Ann Rheum Dis 61(3):199-200. doi: 10.1136/ard.61.3.199. (PMID: 11830422)

Kanakis M, Petrou P, Lourida G, Georgalas I (2022) Erdheim-Chester disease: a comprehensive review from the ophthalmologic perspective. Surv Ophthalmol 67(2):388-410. doi: 10.1016/j.survophthal.2021.05.013. (PMID: 34081930)

Lodhi U, Sarmast U, Khan S, Yaddanapudi K (2016) Multisystem Radiologic Manifestations of Erdheim-Chester Disease. Case Rep Radiol 2016:2670495. doi: 10.1155/2016/2670495. (PMID: 27340583)

Jois B, Ananthasivan R, Rawat PRVS, Rakshit S (2021) Role of 18F-FDG PET/CT in Erdheim-Chester Disease in the Era of Multimodality Imaging. Indian J Radiol Imaging 31(3):729-734. doi: 10.1055/s-0041-1736164. (PMID: 34790325)

Boyd LC, O'Brien KJ, Ozkaya N, Lehky T, Meoded A, Gochuico BR, Hannah-Shmouni F, Nath A, Toro C, Gahl WA, Estrada-Veras JI, Dave RH (2020) Neurological manifestations of Erdheim-Chester Disease. Ann Clin Transl Neurol 7(4):497-506. doi: 10.1002/acn3.51014. (PMID: 32227455)

Mamlouk MD, Aboian MS, Glastonbury CM (2017) Case 245: Erdheim-Chester Disease. Radiology 284(3):910-917. doi: 10.1148/radiol.2017141151. (PMID: 28825890)

Drier A, Haroche J, Savatovsky J, Godenèche G, Dormont D, Chiras J, Amoura Z, Bonneville F (2010) Cerebral, facial, and orbital involvement in Erdheim-Chester disease: CT and MR imaging findings. Radiology 255(2):586-94. doi: 10.1148/radiol.10090320. (PMID: 20413768)

Samaniego-Toro D, González V, Llauradó Gayete A, Gabaldón Domínguez MA, Hernández-Vara J (2022) The Dentate Nucleus Is the Clue: Erdheim-Chester Disease as a Cause of Cerebellar Syndrome. Mov Disord Clin Pract 9(Suppl 2):S17-S20. doi: 10.1002/mdc3.13526. (PMID: 36118514)

Wang F, Cao X, Niu N, Zhang Y, Wang Y, Feng F, Jin Z (2019) Multisystemic Imaging Findings in Chinese Patients With Erdheim-Chester Disease. AJR Am J Roentgenol 213(6):1179-1186. doi: 10.2214/AJR.19.21523. (PMID: 31532257)

Merritt H, Pfeiffer ML, Richani K, Phillips ME (2016) Erdheim-Chester disease with orbital involvement: Case report and ophthalmic literature review. Orbit 35(4):221-6. doi: 10.1080/01676830.2016.1176211. (PMID: 27322549)

Kumar P, Singh A, Gamanagatti S, Kumar S, Chandrashekhara SH (2018) Imaging findings in Erdheim-Chester disease: what every radiologist needs to know. Pol J Radiol 83:e54-e62. doi: 10.5114/pjr.2018.73290. (PMID: 30038679)

Villatoro-Villar M, Bold MS, Warrington KJ, Crowson CS, Goyal G, Shah M, Go RS, Koster MJ (2018) Arterial involvement in Erdheim-Chester disease: A retrospective cohort study. Medicine (Baltimore) 97(49):e13452. doi: 10.1097/MD.0000000000013452. (PMID: 30544428)

Wittenberg KH, Swensen SJ, Myers JL (2000) Pulmonary involvement with Erdheim-Chester disease: radiographic and CT findings. AJR Am J Roentgenol 174(5):1327-31. doi: 10.2214/ajr.174.5.1741327. (PMID: 10789787)

Sezer H, Aygün MS, Armutlu A, Acar Ö, Falay FO, Yazici D, Deyneli O, Alagöl F (2018) Erdheim-chester disease:

Case report with testes involvement and review of literature. Urol Case Rep 18:19-21. doi: 10.1016/j.eucr.2018.02.007. (PMID: 29686965)

Figure 1

a

Description: Xanthelasma involving the right eye, indicated by the thick blue arrow. **Origin:** © Department of Radiology, Amala Institute of Medical Sciences, Kerala University of Health Sciences, India, 2023

Figure 2

a

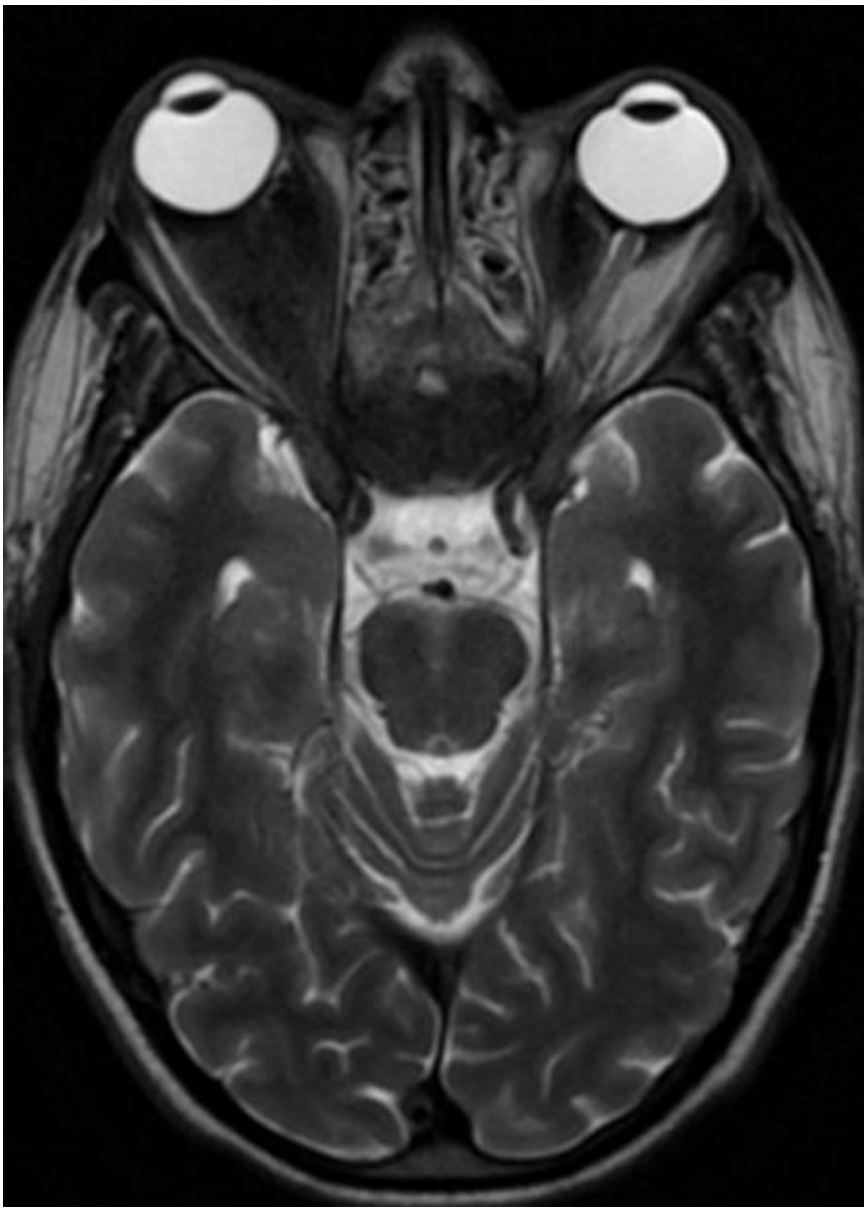

Description: Axial T2 FSE (Figure 2a) and axial post-contrast T1W (Figure 2b) images demonstrating hypointense, heterogeneously enhancing soft tissue thickening (black arrows) involving bilateral extraocular muscles, bilateral intraconal spaces, resulting in right-sided proptosis, along with encasement and compression of bilateral optic nerves. Axial post-contrast T1W image (2b) reveals an enhancing focus in the peridentate nucleus region of the left cerebellar hemisphere (thick blue arrow).
Origin: © Department of Radiology, Amala Institute of Medical Sciences, Kerala University of Health Sciences, India, 2023

b

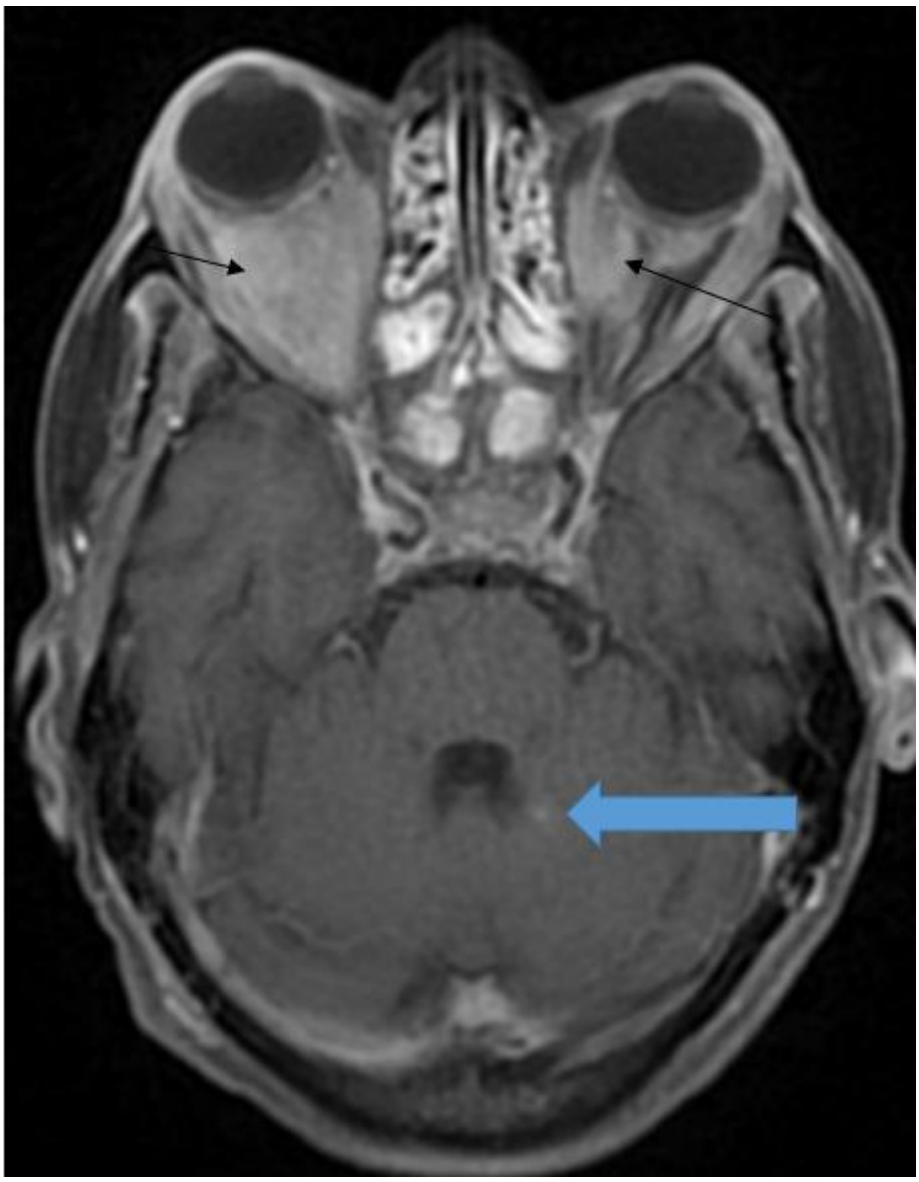

Description: Axial T2 FSE (Figure 2a) and axial post-contrast T1W (Figure 2b) images demonstrating hypointense, heterogeneously enhancing soft tissue thickening (black arrows) involving bilateral extraocular muscles, bilateral intraconal spaces, resulting in right-sided proptosis, along with encasement and compression of bilateral optic nerves. Axial post-contrast T1W image (2b) reveals an enhancing focus in the peridentate nucleus region of the left cerebellar hemisphere (thick blue arrow).
Origin: © Department of Radiology, Amala Institute of Medical Sciences, Kerala University of Health Sciences, India, 2023

c

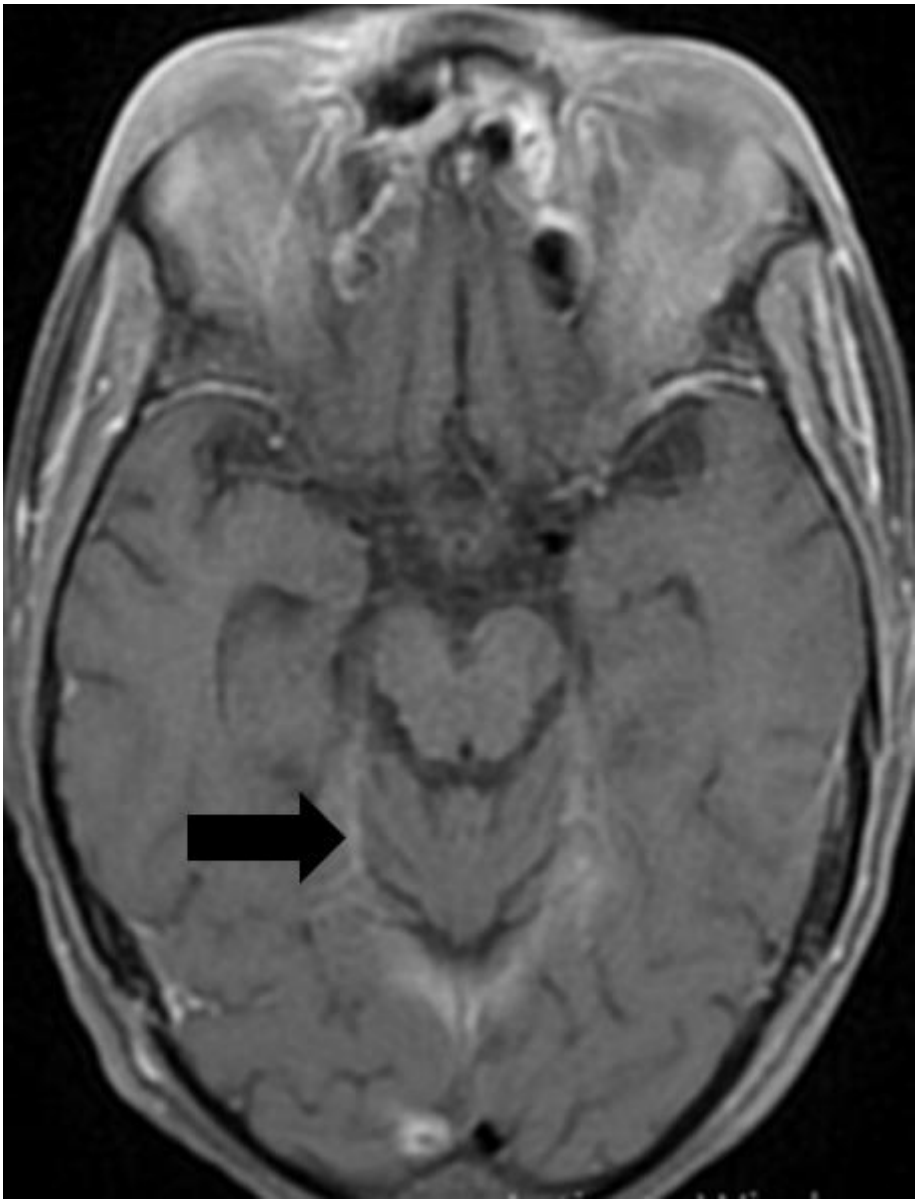

Description: Axial post-contrast T1 images exhibit enhancement and thickening in the bilateral tentorium cerebelli (thick black arrow). **Origin:** © Department of Radiology, Amala Institute of Medical Sciences, Kerala University of Health Sciences, India, 2023

Figure 3

a

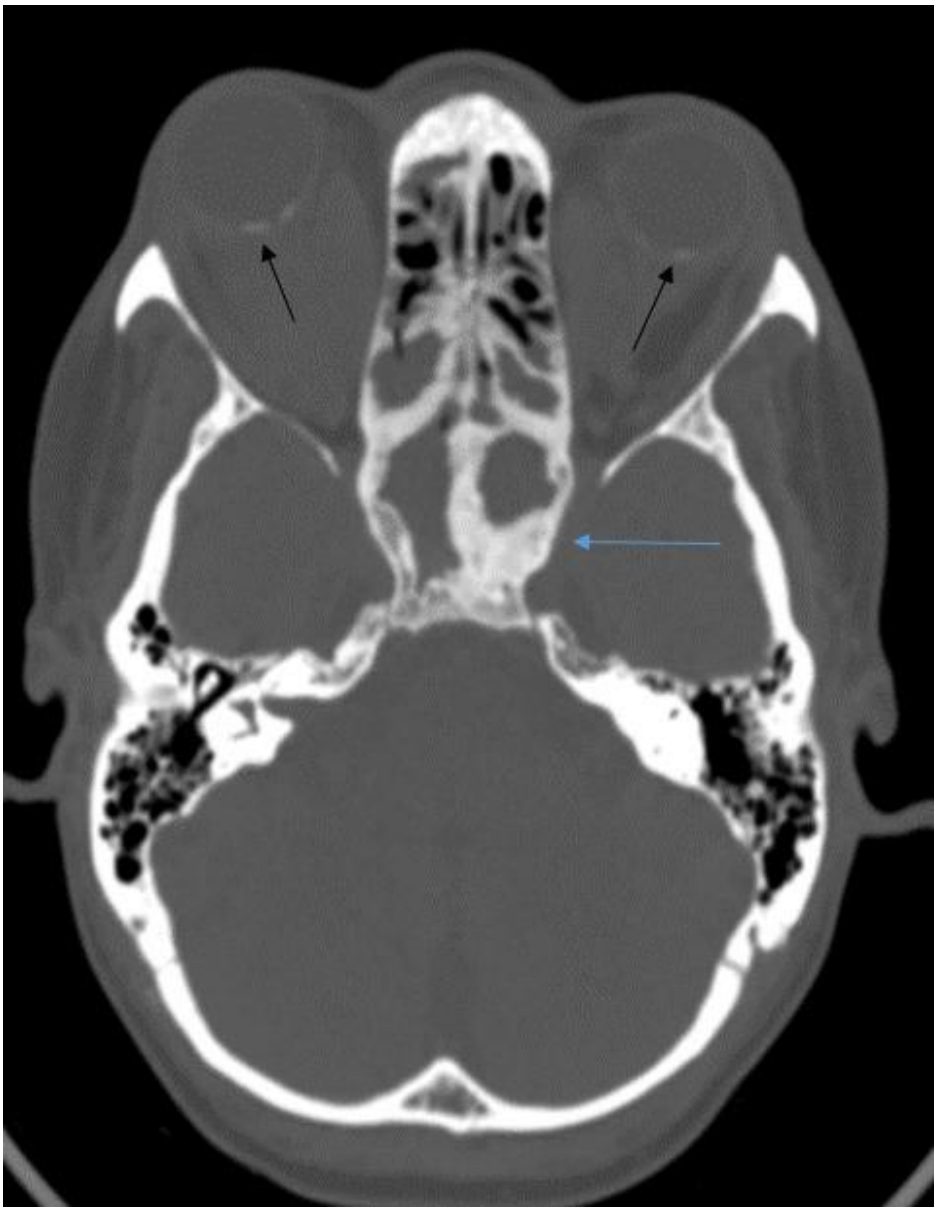

Description: Axial CT section reveals sclerotic bone thickening and expansion of bilateral ethmoidal and sphenoidal sinuses (thin blue arrow). Additionally, calcification is noted in the posterior chamber of bilateral globes in the region of the optic nerve insertion (thick black arrow). **Origin:** © Department of Radiology, Amala Institute of Medical Sciences, Kerala University of Health Sciences, India, 2023

b

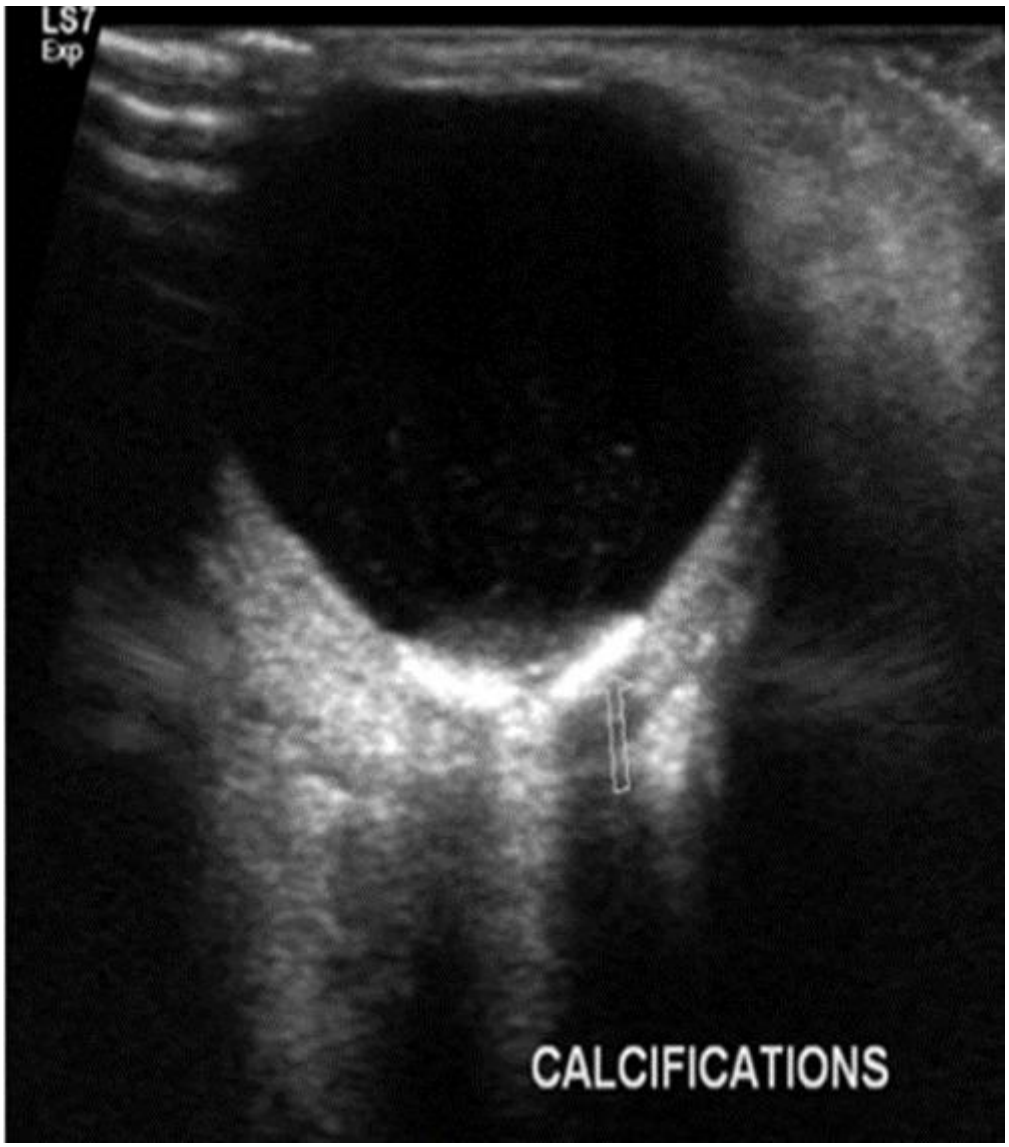

Description: Ocular ultrasound of the right eye demonstrates an echogenic focus in the region of the optic nerve head, suggestive of optic nerve drusens (white arrow). **Origin:** © Department of Radiology, Amala Institute of Medical Sciences, Kerala University of Health Sciences, India, 2023

Figure 4

a

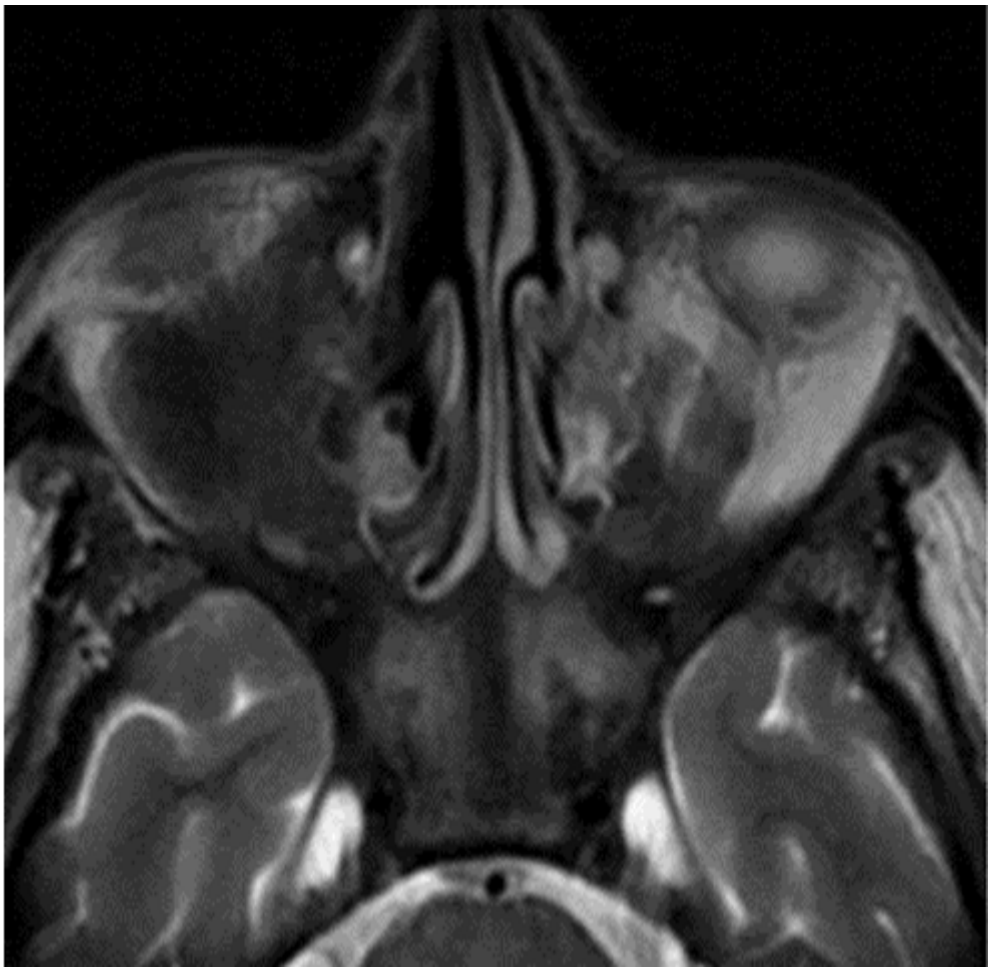

Description: Axial T2 images showing hypointense soft tissue and wall thickening of (4a) bilateral ethmoidal (thin white arrow), bilateral sphenoidal (thin black arrow), (4c) bilateral maxillary sinuses with heterogenous post-contrast enhancement (thick blue arrow) in axial post contrast images (Figures 4b, 4d). **Origin:** © Department of Radiology, Amala Institute of Medical Sciences, Kerala University of Health Sciences, India, 2023

b

Description: Axial T2 images showing hypointense soft tissue and wall thickening of (4a) bilateral ethmoidal (thin white arrow), bilateral sphenoidal (thin black arrow), (4c) bilateral maxillary sinuses with heterogenous post-contrast enhancement (thick blue arrow) in axial post contrast images (Figures 4b, 4d). **Origin:** © Department of Radiology, Amala Institute of Medical Sciences, Kerala University of Health Sciences, India, 2023

c

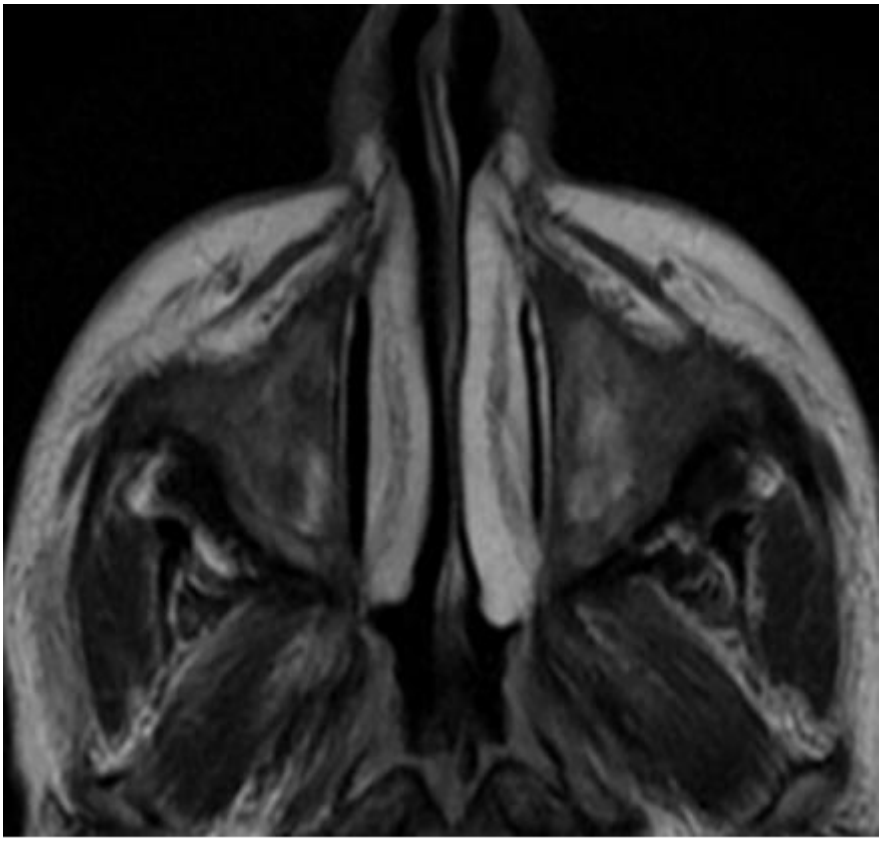

Description: Axial T2 images showing hypointense soft tissue and wall thickening of (4a) bilateral ethmoidal (thin white arrow), bilateral sphenoidal (thin black arrow), (4c) bilateral maxillary sinuses with heterogenous post-contrast enhancement (thick blue arrow) in axial post contrast images (Figures 4b, 4d). **Origin:** © Department of Radiology, Amala Institute of Medical Sciences, Kerala University of Health Sciences, India, 2023

d

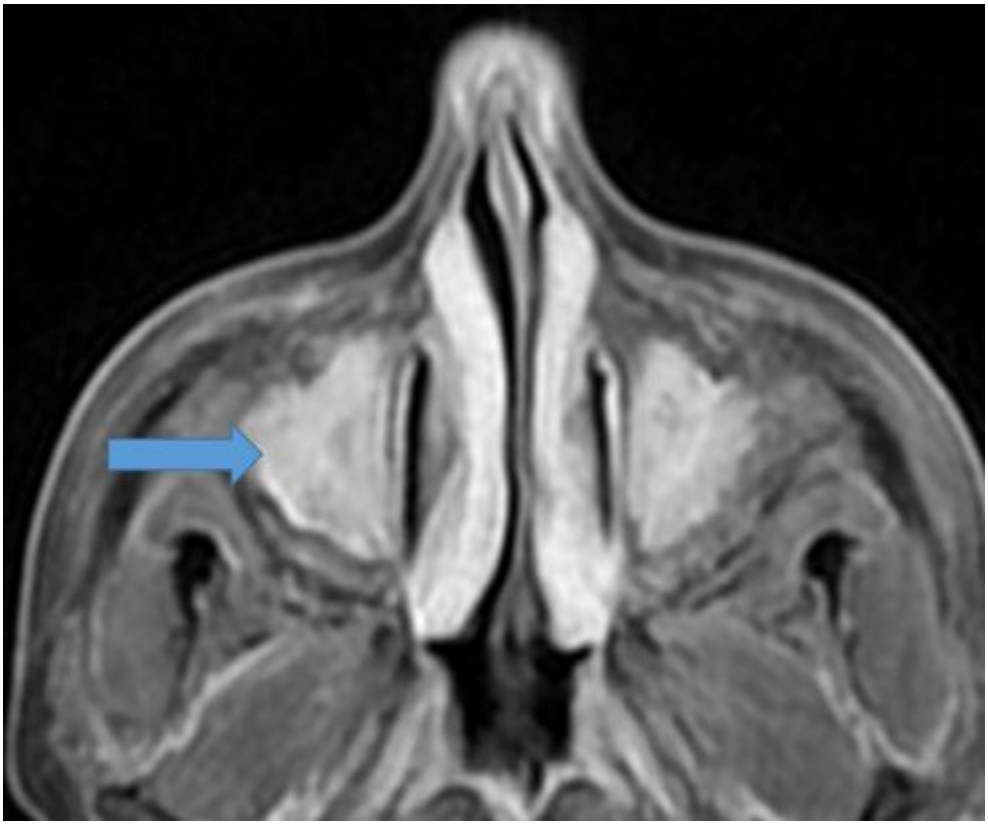

Description: Axial T2 images showing hypointense soft tissue and wall thickening of (4a) bilateral ethmoidal (thin white arrow), bilateral sphenoidal (thin black arrow), (4c) bilateral maxillary sinuses with heterogenous post-contrast enhancement (thick blue arrow) in axial post contrast images (Figures 4b, 4d). **Origin:** © Department of Radiology, Amala Institute of Medical Sciences, Kerala University of Health Sciences, India, 2023

Figure 5

a

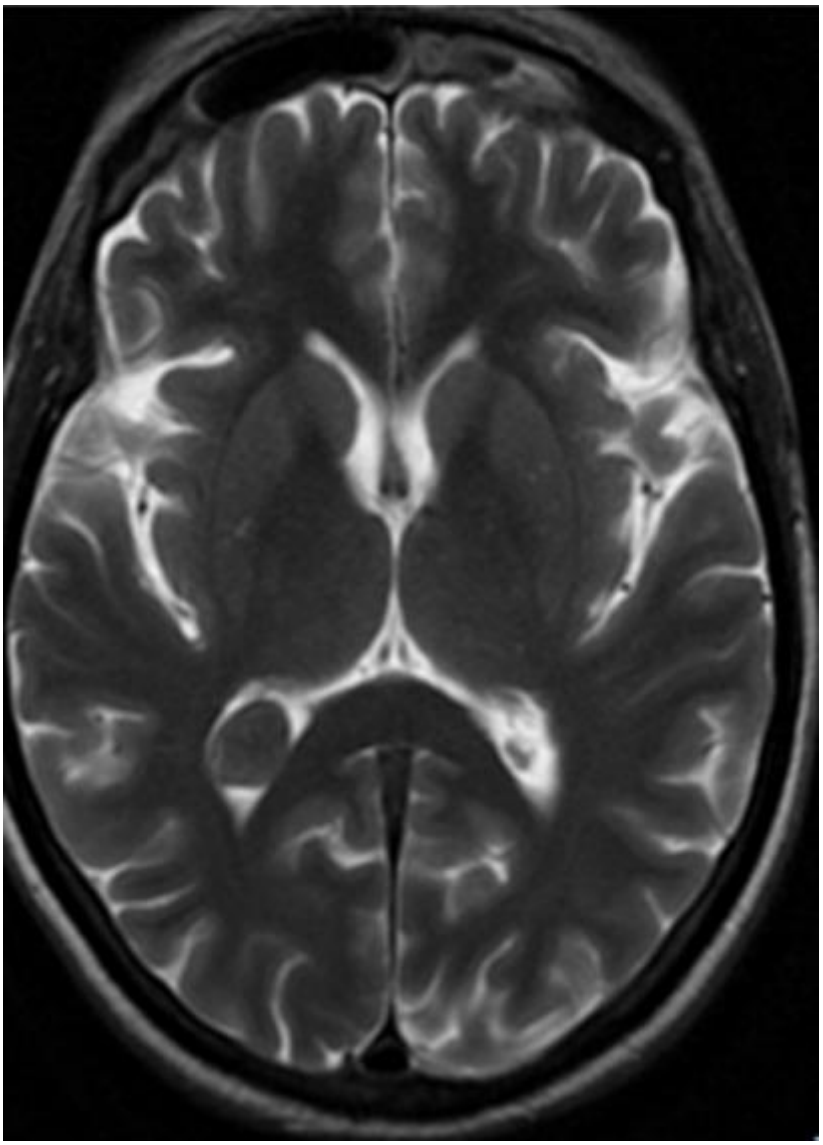

Description: Axial T2 images depict a hypointense lobulated lesion with increased FDG uptake involving the choroid plexus in the occipital horn of the right lateral ventricle (thick black arrow). **Origin:**

b

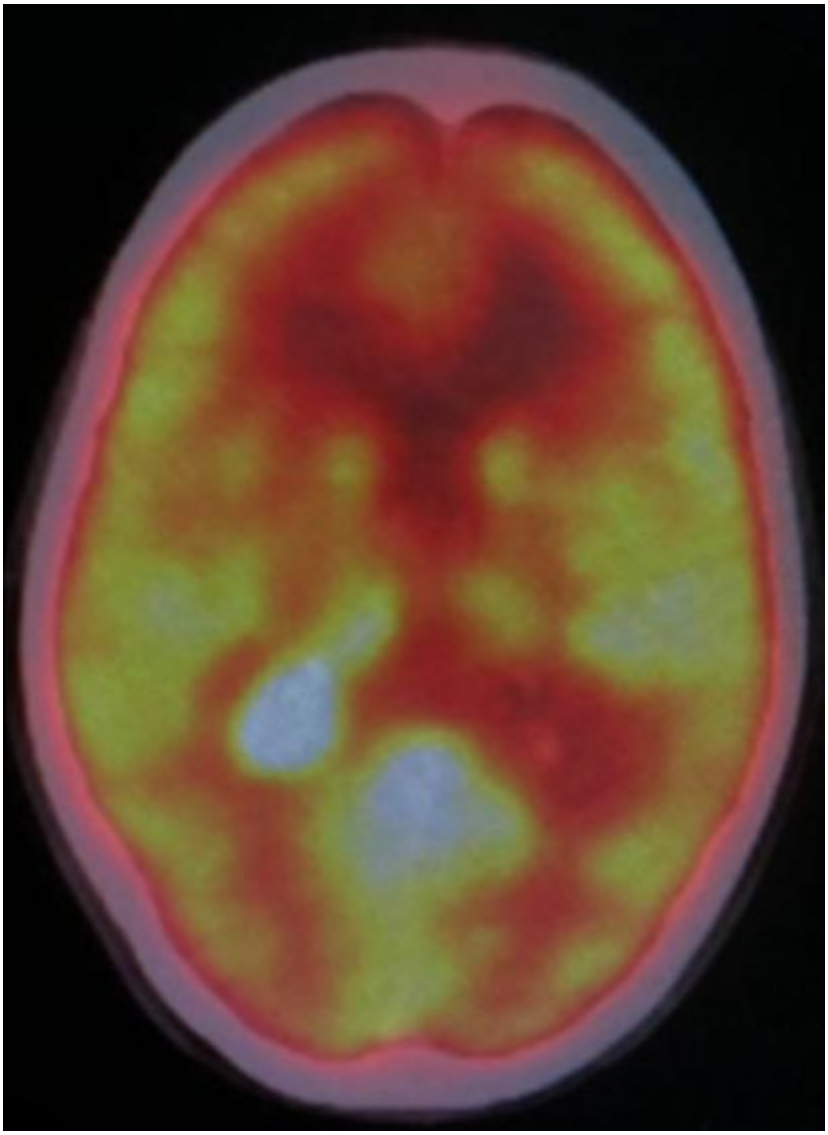

Description: Axial T2 images depict a hypointense lobulated lesion with increased FDG uptake involving the choroid plexus in the occipital horn of the right lateral ventricle (thick black arrow).**Origin:**

c

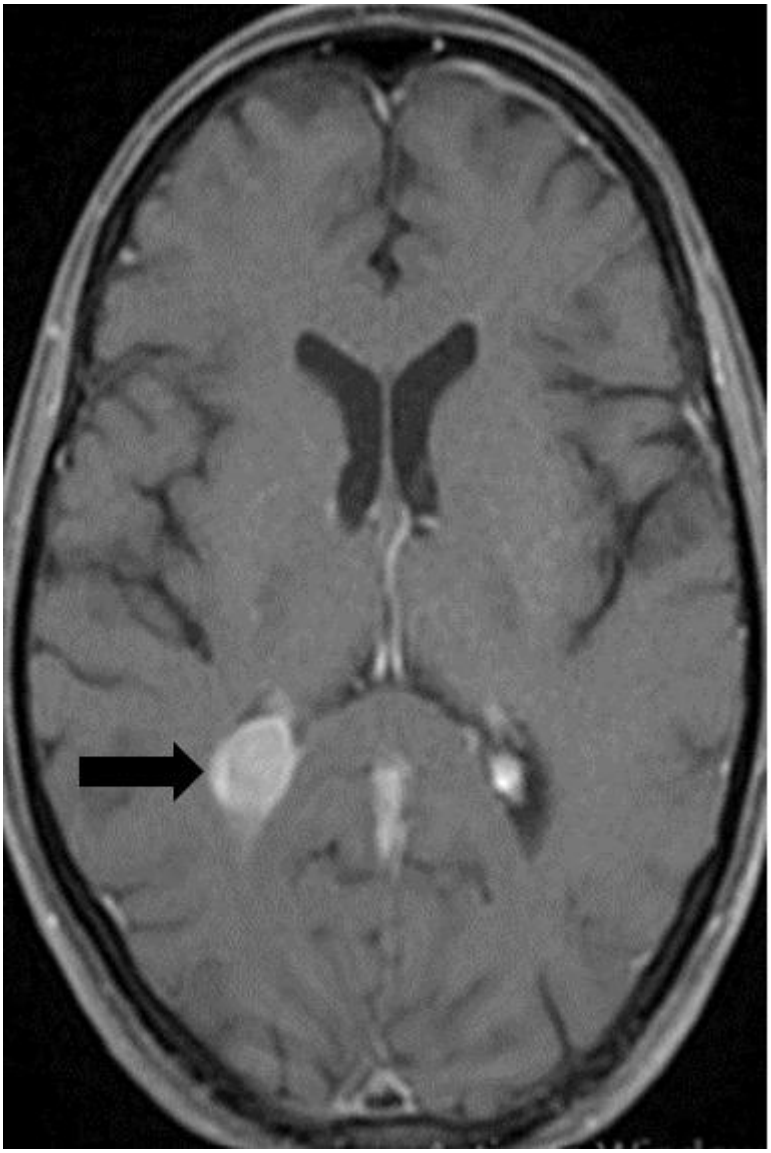

Description: Axial post-contrast T1 images show near-homogeneous post-contrast enhancement of the same lesion. **Origin:** © Department of Radiology, Amala Institute of Medical Sciences, Kerala University of Health Sciences, India, 2023

Figure 6

a

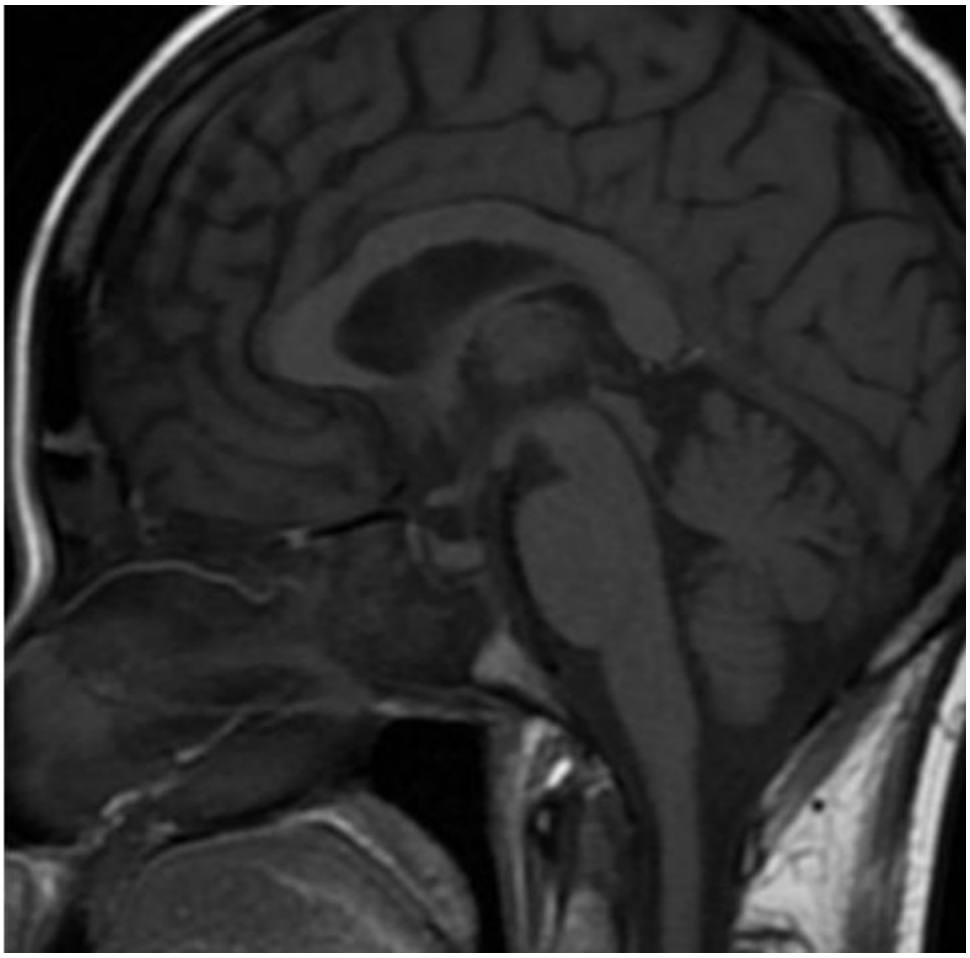

Description: Sagittal non-contrast T1 image showing absence of posterior pituitary bright spot. **Origin:** © Department of Radiology, Amala Institute of Medical Sciences, Kerala University of Health Sciences, India, 2023

Figure 7

a

Description: USG neck showing perivascular thickening in right carotid bulb. **Origin:** © Department of Radiology, Amala Institute of Medical Sciences, Kerala University of Health Sciences, India, 2023

Figure 8

a

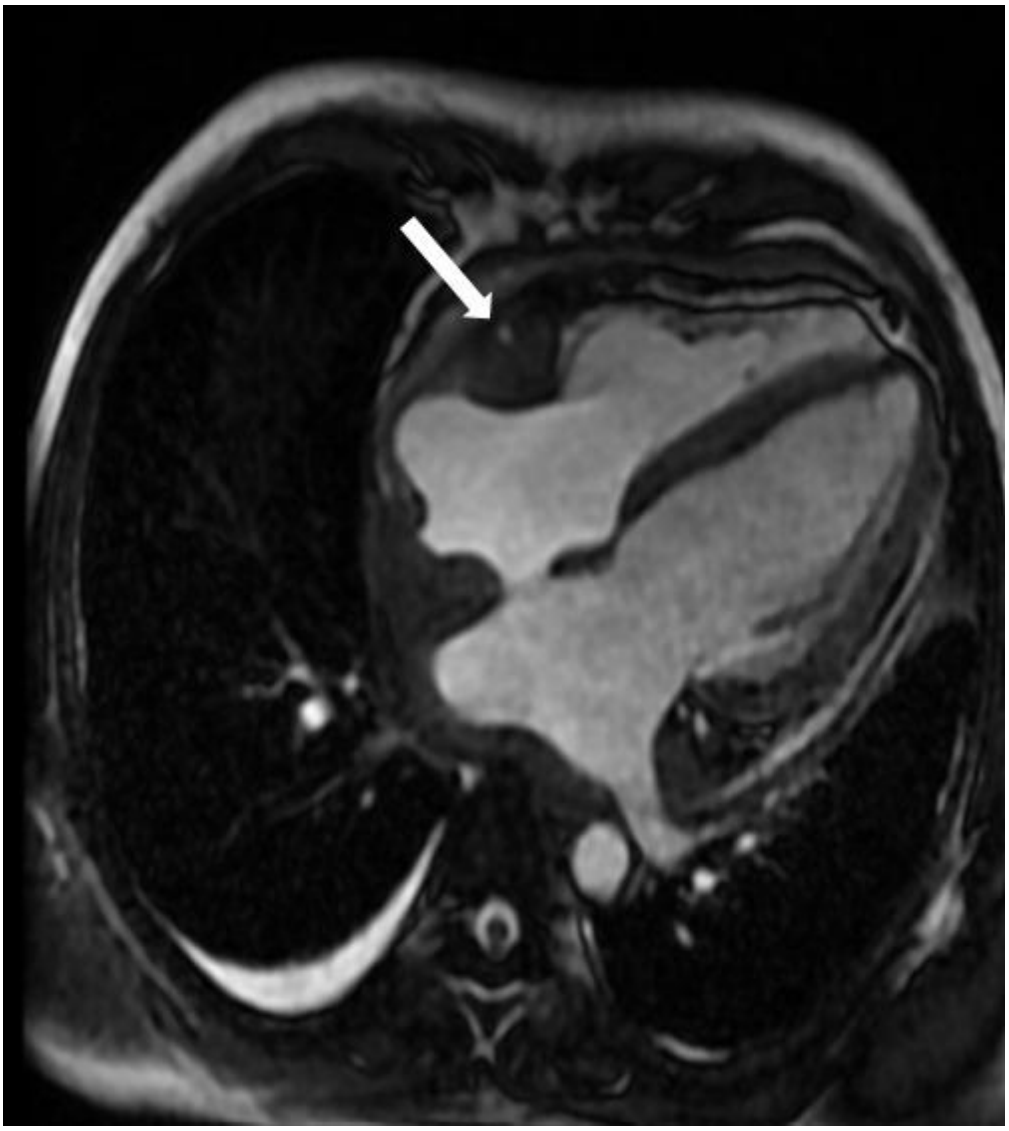

Description: 4H FIESTA CINE sequence displays soft tissue thickening involving walls of both atria, both atrioventricular groove encasing right coronary artery (thick white arrow) and left circumflex artery (thick blue arrow), with mild extension into epicardial surface of both ventricles in basal region showing Figure 8b: post-contrast enhancement in late enhancement cardiac MR sequences along with diffuse pericardial thickening and mild pericardial effusion (thick white arrow). **Origin:** © Department of Radiology, Amala Institute of Medical Sciences, Kerala University of Health Sciences, India, 2023

b

Description: 4H FIESTA CINE sequence displays soft tissue thickening involving walls of both atria, both atrioventricular groove encasing right coronary artery (thick white arrow) and left circumflex artery (thick blue arrow), with mild extension into epicardial surface of both ventricles in basal region showing Figure 8b: post-contrast enhancement in late enhancement cardiac MR sequences along with diffuse pericardial thickening and mild pericardial effusion (thick white arrow). **Origin:** © Department of Radiology, Amala Institute of Medical Sciences, Kerala University of Health Sciences, India, 2023

Figure 9

a

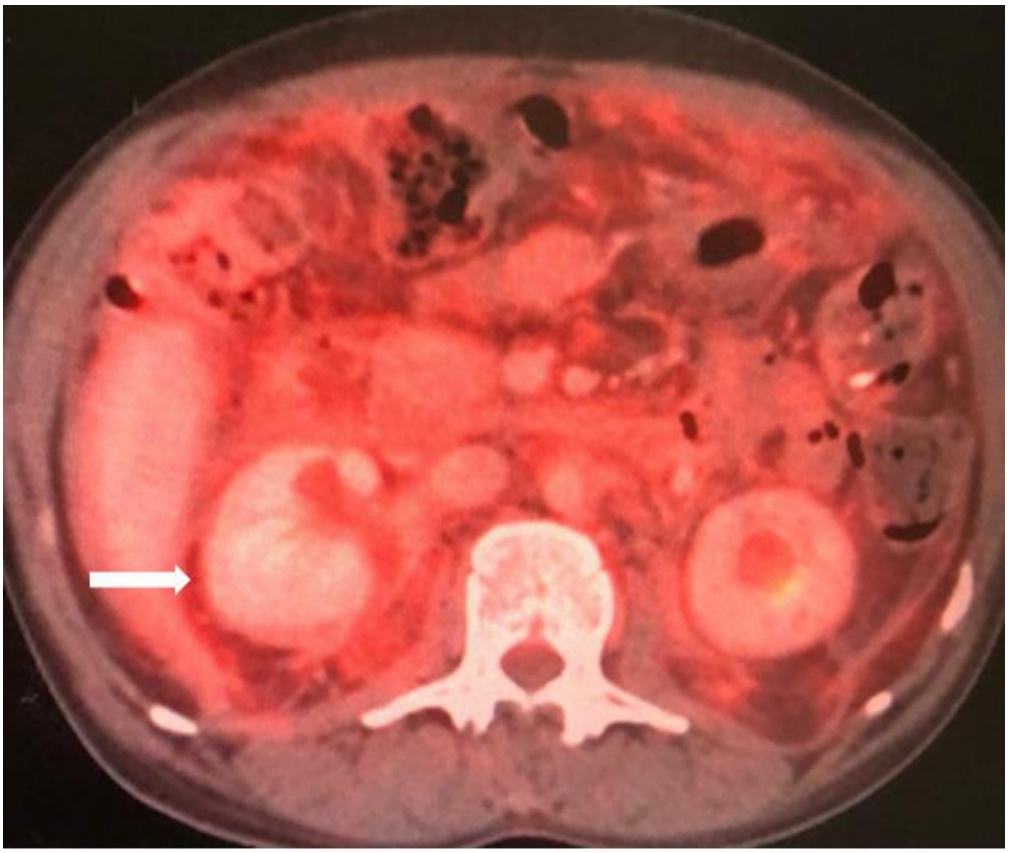

Description: Axial FDG PET-CT images reveal mildly FDG avid diffuse peritoneal thickening and omental fat stranding. There is diffuse retroperitoneal soft tissue thickening encasing the kidneys (thick white arrow), adrenals and major vessels. **Origin:** © Department of Radiology, Amala Institute of Medical Sciences, Kerala University of Health Sciences, India, 2023

b

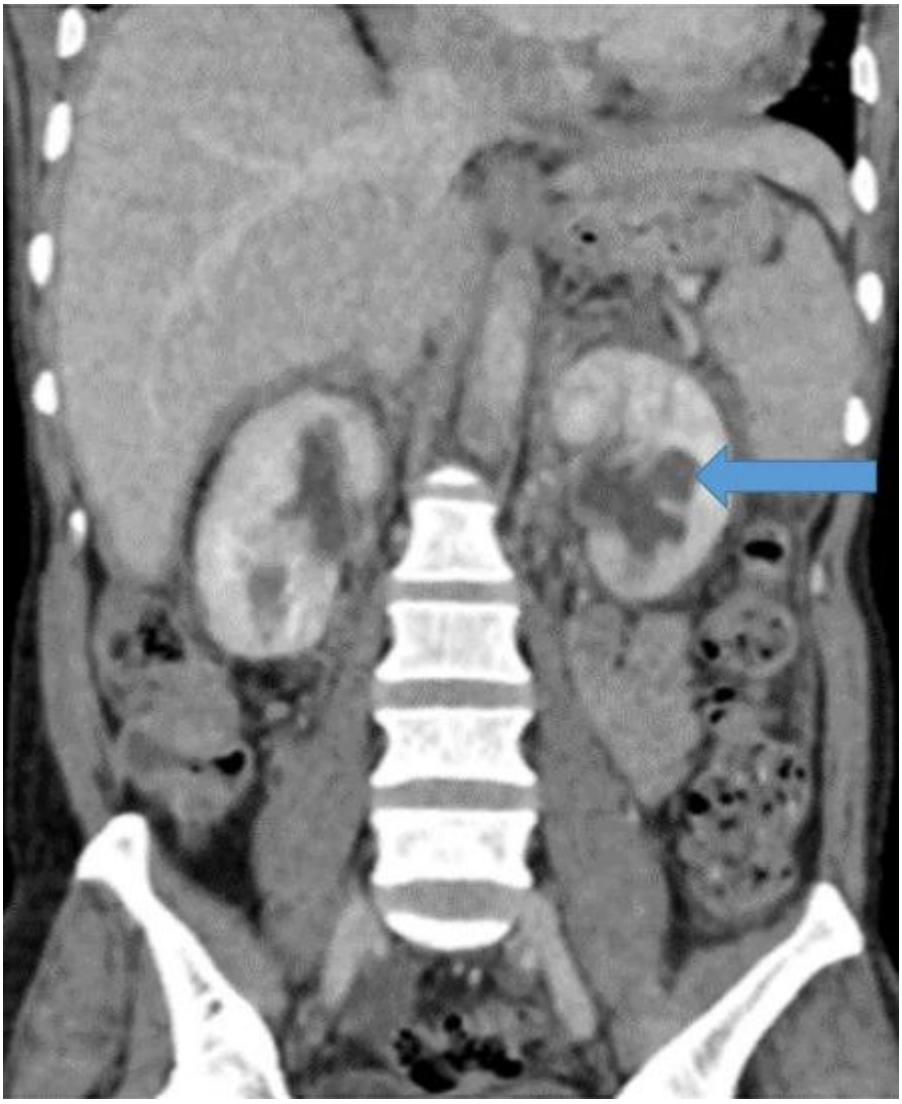

Description: Coronal CT images display symmetric infiltration of bilateral perirenal and posterior pararenal spaces with bilateral moderate hydroureteronephrosis (thick blue arrow). **Origin:** © Department of Radiology, Amala Institute of Medical Sciences, Kerala University of Health Sciences, India, 2023

Figure 10

a

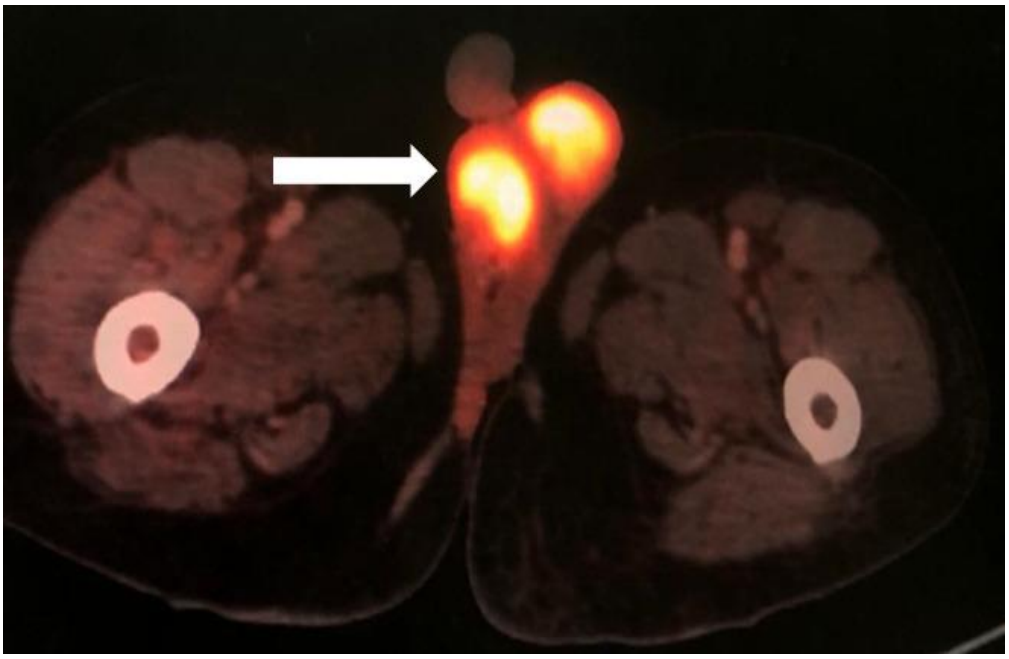

Description: Axial FDG PET-CT image exhibits intense FDG uptake in bilateral testis (thick white arrow). **Origin:** © Department of Radiology, Amala Institute of Medical Sciences, Kerala University of Health Sciences, India, 2023

Figure 11

a

Description: Anterior-posterior (AP) radiographs of bilateral knee joints reveal bilateral symmetrical predominant metadiaphyseal osteosclerosis and cortical thickening (thick blue arrow) in bilateral distal femur and proximal tibia. **Origin:** © Department of Radiology, Amala Institute of Medical Sciences, Kerala University of Health Sciences, India, 2023

b

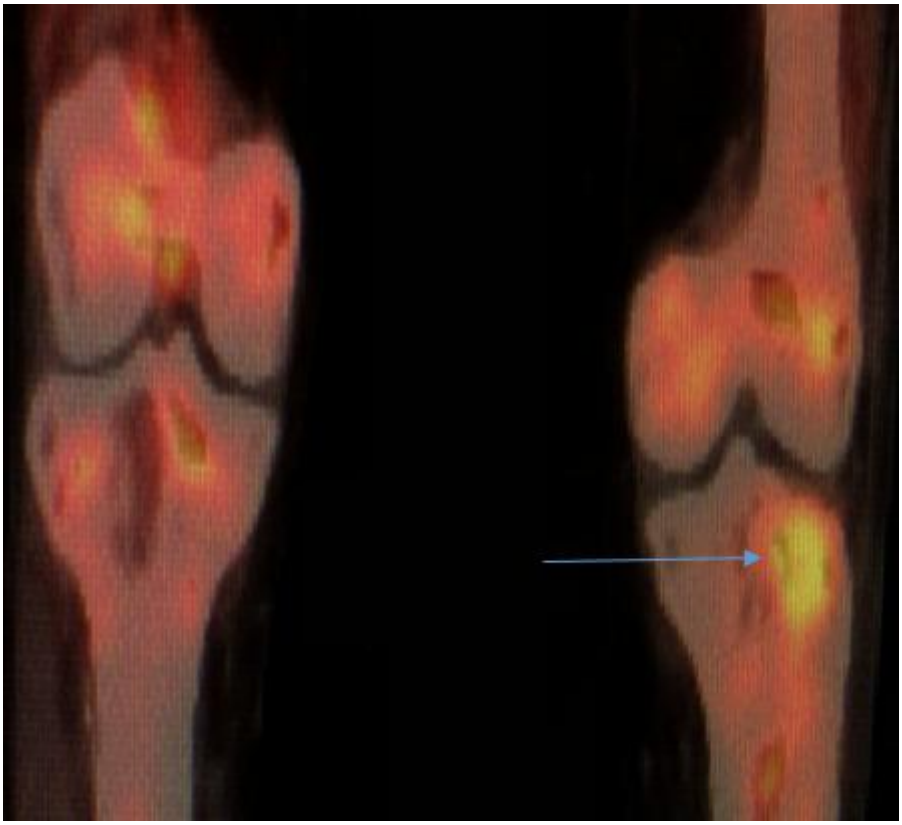

Description: Coronal FDG PET-CT images of knee demonstrate 18F-FDG avid (thin blue arrow) soft tissue thickening in bilateral knee joints. **Origin:** © Department of Radiology, Amala Institute of Medical Sciences, Kerala University of Health Sciences, India, 2023